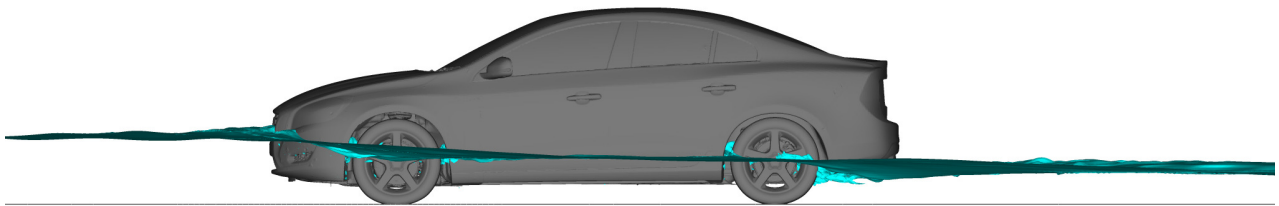


CHALMERS



Numerical Computation of Vehicle Wading

A Study Using the VOF Method

Master's thesis in Fluid Dynamics

SHAYAN RAHAT VARNOUSFADERANI

Department of Applied Mechanics

Division of Fluid Dynamics

CHALMERS UNIVERSITY OF TECHNOLOGY

Göteborg, Sweden 2013

Master's thesis 2013:71

MASTER'S THESIS IN FLUID DYNAMICS

Numerical Computation of Vehicle Wading

A Study Using the VOF Method

SHAYAN RAHAT VARNOUSFADERANI

Department of Applied Mechanics
Division of Fluid Dynamics
CHALMERS UNIVERSITY OF TECHNOLOGY
Göteborg, Sweden 2013

Numerical Computation of Vehicle Wading
A Study Using the VOF Method
SHAYAN RAHAT VARNOUSFADERANI

© SHAYAN RAHAT VARNOUSFADERANI, 2013

Master's thesis 2013:71
ISSN 1652-8557
Department of Applied Mechanics
Division of Fluid Dynamics
Chalmers University of Technology
SE-412 96 Göteborg
Sweden
Telephone: +46 (0)31-772 1000

Cover:
Side view of a car CAD model with the calculated water surface isolated and shown.

Chalmers Reproservice
Göteborg, Sweden 2013

Numerical Computation of Vehicle Wading
A Study Using the VOF Method
Master's thesis in Fluid Dynamics
SHAYAN RAHAT VARNOUSFADERANI
Department of Applied Mechanics
Division of Fluid Dynamics
Chalmers University of Technology

ABSTRACT

A method was developed for the numerical calculation of vehicle wading in the commercial software Fluent. The VOF method was used for modeling of the two-phase flow. This method combines the two phases, air and water, into a single fluid with variable properties. The results were examined to gain a better understanding of the characteristics of the velocity field and the variation of the wading-line height on the car. The results show qualitative agreement with tests carried out at the Hällered test facility. Comprehensive quantitative comparisons were not attempted as measurement of the relevant variables requires upgrading of the testing equipment available.

A simplified procedure was also developed for estimating the vertical force on the car and the subsequent height raise. The method neglects dynamic effects and was found to overestimate the force. Yet, the method is useful as a dynamic balance calculation is not currently feasible. Suggestions for improving wading performance evaluation are provided that can build on the work done during this project.

Keywords: CFD, VOF, Multiphase Flows

PREFACE

The current project was carried out at the contamination group within the CFD department at *Volvo Cars Corporation*. A computational method was developed for the calculation of vehicle wading in Fluent. A common task of the CFD department is method development. Method development in this context refers to the establishment of an automated, well-documented procedure for numerical calculation of flow situations that have to be examined repeatedly for many projects.

A simplified procedure was also established for estimation of the upward force acting on the vehicle and the resulting height raise. The simplified procedure was chosen because including such calculations in the CFD method is not currently computationally feasible. The method was found to overestimate the force and the height raise, but an empirically determined term that represents dynamic effects is expected to improve the method without increasing the computational cost. This was not attempted in the current work because of time limitations.

ACKNOWLEDGEMENTS

I would like to thank everyone at the CFD department at Volvo cars for the great time I had while I was there. I am specially thankful to my supervisor, Dragos Moroianu, who helped me throughout the project and from whom I learned a great deal. I am also grateful to my examiner at Chalmers, Håkan Nilsson, for his help and patience with this report. Lastly yet mostly, I am thankful to my great family for their never-ceasing support.

CONTENTS

Abstract	i
Preface	iii
Acknowledgements	iii
Contents	v
1 Introduction	1
1.1 Overview	1
1.2 Relevance	1
1.3 Goals	2
1.4 Outline	2
2 Mathematical Theory	3
2.1 Classification of Multiphase Flows	3
2.1.1 Separated Two-Phase Flows	4
2.2 Surface Methods	4
2.2.1 Height Functions	4
2.2.2 Particles on Interface	4
2.3 Volume Methods	5
2.3.1 Particles in Cells	5
2.3.2 Marker and Cell	6
2.3.3 Volume of Fluid Method	6
2.4 The VOF Method	7
2.4.1 Field Equations Governing The Flow	7
3 Numerical Model	9
3.1 Introduction	9
3.2 Integral Equations of Conservation	9
3.3 Discretization of The Geometry	9
3.4 Discretization Schemes	10
3.5 Boundary Conditions	10
4 Results	11
4.1 Temporal Progression of the Solution	11
4.2 Quasi-steady Solution	11
4.3 Forces	17
5 Conclusion	20
5.1 CFD Method	20
5.2 Forces	20
5.3 Testing	20
References	21

1 Introduction

The present chapter introduces the subject of this report. *Wading* is defined in the context of automotive engineering, and reasons are given for examining the fluid mechanics involved. The goals of the current project are introduced next. Lastly, an overview of the report is given.

1.1 Overview

Wading, in the context of automotive engineering, refers to the situation where a car is moving through relatively deep water at low velocity. Two common examples are crossing rivers and moving through flooded roads. *Wading* and *fording* are used interchangeably in this regard.

From a fluid mechanics point of view, the situation is characterized by a complex transient phase where a substantial volume of water is set into motion by the entrance of the vehicle into the water. After entrance into the water, the flow is characterized by a bow wave in front of the vehicle and a wading line that is substantially higher on the front section of the vehicle compared to the back, somewhat resembling the flow downstream of a sluice gate. The described situation is not the only flow regime that can happen but, as it is much less taxing on the vehicle, it is the one that the driver *should* aim for when wading is attempted. The flow is considered a free surface flow because of the existence of a deformable interface between water and air. Two contrasting free surface flow regimes can be distinguished based on the ratio of the mean-flow velocity and the surface wave velocity. If the mean flow velocity is lower than the surface wave velocity, waves are able to travel upstream, effectively carrying information about the downstream channel configuration and allowing the flow to gradually adjust itself to changes in channel geometry. Such a flow is classified as a sub-critical flow. In contrast, when the mean flow velocity is greater than the surface wave velocity, the waves are inhibited from traveling upstream, leading to sudden adaptations to changes in the channel geometry, e.g. hydraulic jumps. The Froude number is a dimensionless number used to classify free surface flows:

$$Fr = \frac{v}{c} \quad (1.1)$$

where v is the characteristic velocity of the flow and c is the characteristic surface wave velocity. Thus it follows that Froude numbers less than one indicate sub-critical flows and those greater than one indicate super-critical flows.

There are many important flow situations that can potentially compromise the safe and reliable operation of a vehicle, yet do not conform to the more basic aerodynamic and thermal calculations needed for making the initial design decisions. Examples include the deposition of snow on the air intake and wind-shield, splashing of water inside the engine bay when the vehicle passes a shallow pool of water and, the subject of this report, vehicle wading. These flows are commonly grouped under the term *contamination* attributes.

1.2 Relevance

Although wading is not the normal operating condition for a vehicle, it is nonetheless a condition that the vehicle should be able to endure. There are many challenges facing a car when wading. Some of these challenges are as follows:

- Entry of water into the air intake. If significant amounts of water enter the air intake, some of the water could subsequently enter the cylinder. Entrance of water into the cylinder, water being nearly incompressible and having a specific heat orders of magnitude larger than that of the fuel-air mixture, would most likely result in damaging critical components within the engine beyond repair.
- With the ever increasing use of electronics within cars, keeping these components working is another major challenge.
- Resulting from the large upward-directed force exerted on the car, the vehicle becomes much less stable and can be washed downstream or toppled by a transverse wave of water.
- Due to the presence of *breathers* on gearboxes and differentials, leaking of water inside these components through the breather can cause problems in a longer time-span.

Due to these reasons, and many more, evaluation of the wading performance of a vehicle is an important task in the development of new models. To this end, estimates of the position of the wading line on the vehicle and of the forces exerted on the car can provide valuable information.

Before the computational evaluation of wading performance of a vehicle became feasible, this was done by physical testing of the prototypes at different stages of development. In fact, this method is still the more reliable method and is an indispensable tool in the development of new cars. However, with the significant increase in the capabilities of available hardware and software to compute complex flows, it is justifiable to shift some of the work to virtual testing because of its many advantages, some of which will be enumerated in the next section.

1.3 Goals

Wading tests have been carried out previously to ensure meeting expectations. But a CFD method for carrying out wading calculations early during the development phase for a new vehicle offers many benefits. For example, potentially serious flaws could be detected and resolved earlier in a project, avoiding a later revelation which could be much more costly to correct. Also of significant advantage, is the comparable ease with which the conditions of a virtual test can be changed by simply adjusting the relevant parameters in the computer model. Thus the overall goal of this project was incorporation of wading performance evaluation into CAE, thus reducing the need for, and augmenting, physical testing. This goal was defined in terms of a number of deliverables. These are listed below:

- Development of a method for wading calculations
- Suggestion of a way for estimating the vehicle height rise during wading.

In order to build on experience gained from successful simulations and increase efficiency for project-critical calculations, *method development* is a common goal in industrial CFD calculations. This involves arriving at a standardized, well documented procedure for doing a specific calculation that is preferably automated to the maximum extent possible. Consequently, the current project's main goal was to develop a method for performing wading calculations that can be reliably used for future projects.

Additionally, a vehicle experiences a substantial change in the balance of the suspension system during wading. Estimation of this change in suspension system balance during wading is also of great practical interest. However, direct incorporation of such estimates in the CFD calculation method would increase its computational cost to such an extent that it would render it infeasible with the currently available resources. Subsequently, an alternative, less resource-intensive way for making such estimates was sought. A less sophisticated method was chosen in which only the static buoyancy force was considered to cause the rise in the suspension system.

1.4 Outline

Chapter 2 describes the mathematical formulation of the problem in terms of field equations. Chapter 3 describes the discretized form of the field equations as they are used in the numerical calculations. Chapter 4 presents the results of the numerical solution and, lastly, Chapter 5 summarizes the project and suggests some possible paths for further work on the subject.

2 Mathematical Theory

Although single phase formulations of free surface flows are possible, e.g. potential free surface flow theory, vehicle wading was modeled as a multiphase flow in the current project. Multiphase flow refers to a situation where the domain contains two or more distinct phases. Multiphase flows challenge the engineer with a multitude of complex phenomena over a very wide range of time and length scales. Based on the identifying characteristics of different fluid/phase combinations and flow regimes, numerous different mathematical models have been devised over the years to solve problems in multiphase flows.

This chapter starts with a brief overview of some of the ways in which multiphase flows are categorised and goes on to explain in some detail where in this categorization the current problem best fits and the specific mathematical model adopted; i.e. the volume of fluid method.

2.1 Classification of Multiphase Flows

Multiphase flow refers to situations where the flow domain is occupied by two or more phases that are separated at a scale much larger than the molecular scale. It is essential that the phases, which can include more than one fluid phase, remain distinguishable at a macroscopic scale; thus differentiating multiphase flows from multicomponent flows where the distinction between the constituents vanishes as one zooms out from the molecular scale.

Limiting the discussion to two phases, flows are classified based on the phases present in the flow and the structure of the interface between the phases. Depending on the geometry of the interface, two-phase flows are broadly classified as separated, transitional or mixed, and dispersed. Within these three categories, flows are further subdivided based on the state of the phases and the flow regime. Figure 2.1 [15] illustrates the classification of two-phase flows.

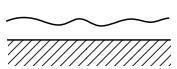
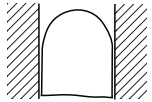
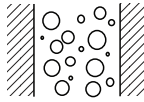
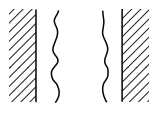
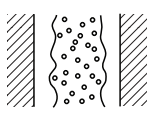
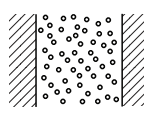

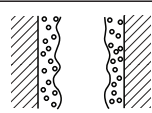
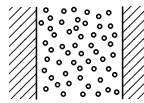
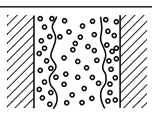
Separated flows	Mixed or Transitional flows	Dispersed flows
 <p>Film flow</p> <p>Liquid film in gas Gas film in liquid</p>	 <p>Cap, Slug or Churn-turbulent flow</p> <p>Gas pocket in liquid</p>	 <p>Bubbly flow</p> <p>Gas bubbles in liquid</p>
 <p>Annular flow</p> <p>Liquid core with gas film Gas core with liquid film</p>	 <p>Droplet annular flow</p> <p>Gas core with droplets and liquid film</p>	 <p>Droplet flow</p> <p>Liquid droplets in gas</p>
 <p>Jet flow</p> <p>Liquid jet in gas Gas jet in liquid</p>	 <p>Bubbly annular flow</p> <p>Gas bubbles in liquid film with gas core</p>	 <p>Particulate flow</p> <p>Solid particles in gas or liquid</p>
	 <p>Bubbly droplet annular flow</p> <p>Gas core with droplets and liquid film with bubbles</p>	

Figure 2.1: *Classification of two-phase flows [14]*

2.1.1 Separated Two-Phase Flows

Considering air and water as two immiscible fluids, the two-phase flow encountered in vehicle wading can be considered a separated gas-liquid flow. Such flows are characterized by a well-defined, sharp interface mostly confined to a small region of the domain. Resolving this sharp interface between the two phases is a necessary requirement for any method proposed for calculating separated flows.

Taking into account the confined nature of the interactions between the two phases, research aimed at modelling separated flows has resulted in the development of a specialized class of methods. In many respects, these methods are different from the Eulerian-Eulerian approach used for modelling many transitional and dispersed flows where the two phases interact throughout the domain and are treated as inter-penetrating continua occupying the same space.

Limiting the discussion to a simple, continuous free surface for the moment, the free surface can be seen as a common, deformable boundary between two separate fluids residing on either side. Consequently, this simplified problem can conceivably be dealt with by imposing kinematic and dynamic boundary conditions on the free surface and solving the resulting moving-boundary, initial value problem. With further simplifications, neglecting viscosity of water and only dealing with the water below the free surface, one arrives at the classical potential surface theory and wave theory [19], [2]. However, these methods cannot be used for problems involving breaking waves and other complex free surface phenomena.

With complex interfaces, more robust methods capable of resolving surface break-up/merging need to be used. In the context of computational fluid dynamics, depending on whether the solution algorithm deals explicitly with the interface or it emerges as part of the solution, methods for modelling separated flows are classified into two categories[8]:

- Surface methods (interface tracking)
- Volume methods (interface capturing)

In surface methods, the *interface* between the two fluids is explicitly tracked. This can be done through a variety of methods. Particles can be assigned to the interface and subsequently followed, the interface can be attached to a mesh surface which is moved with the surface or it can be described as the value of a height function above a certain reference plane.

In contrast, volume methods mark the two *fluids* separated by the interface. This means that the exact position of the interface is not an explicit part of the problem formulation. The two most prominent interface capturing methods are the marker and cell (MAC) method of [11] and the volume of fluid (VOF) method of [12].

2.2 Surface Methods

2.2.1 Height Functions

In this method, the free surface is tracked by making use of a function whose value is equal to the elevation of the free surface above a reference plane. For free surfaces with a simple, continuous topology, this method offers a simple way of keeping track, and evolving with time of the free surface. However, this method has the major limitation that for any point on the reference plane, the free surface can only be located at one height, thus lacking the capability of dealing with complex free surfaces. The method can also be used for closed surfaces, such as droplets, by specifying the location of the free surface relative to a single reference point inside the surface. Figure 2.2.1 depicts the essence of the method.

2.2.2 Particles on Interface

This method marks the interface with a sequence of surface particles and subsequently moves the particles with time with the local velocity. The free surface is approximated by a spline function passing through the marker particles. The method has a number of limitations. Firstly, it is sensitive to the spacing of the particles on the surface and since the particles do not retain their initial spacing, there is a need for continuously adding and deleting marker particles to keep the spacing acceptable. Secondly, as described by [4], the method needs to keep track of the particles in an ordered sequence. This further complicates the process of adding and deleting marker particles as the order of the particles needs to be restored. Lastly, application of the method

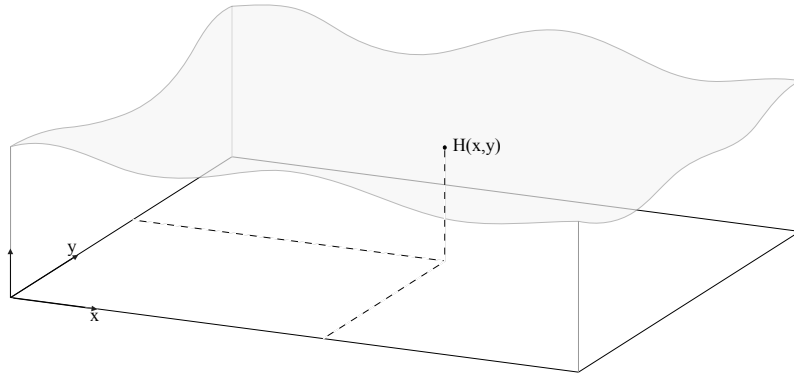


Figure 2.2: *Height functions.*

to three-dimensional cases is quite problematic as the line segments attaching the markers are replaced with three dimensional surfaces with serious challenges in terms of selecting the points used for each surface and attachment of the surfaces together, among other issues.



Figure 2.3: *Particles on surface method.*

2.3 Volume Methods

2.3.1 Particles in Cells

The particle in cell (PIC) method of [7], uses Lagrangian tracking of a number of *fluid particles* on a fixed Eulerian mesh to solve for the flow field variables. The method is defined by a number of phases for each time-step. First, simplified approximations of the Eulerian field equations are solved to calculate rough estimates of acceleration and velocity at each cell center. Next, the particles are moved according to velocities interpolated from the cell centers. In the third phase, corrections are made to the variables for the cells which

have experienced changes in their composition due to the passing of fluid particles through their boundaries. It should be mentioned that the particles in the PIC method have mass assigned to them and are subsequently used to calculate the properties of the fluid, i.e. density, at each cell center. One of the major disadvantages of this method is the large computational resources necessary when applied to three-dimensional problems.

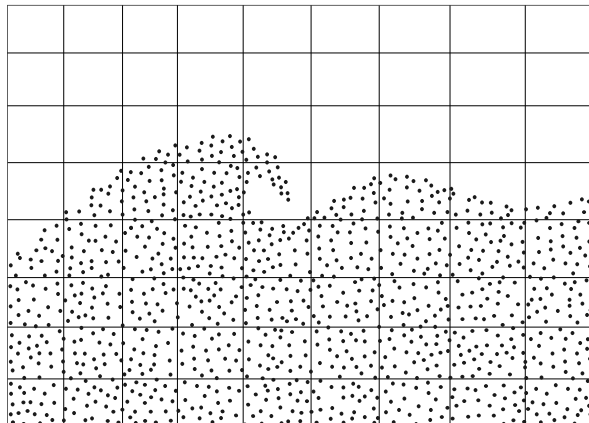


Figure 2.4: *PIC method.*

2.3.2 Marker and Cell

In the marker and cell (MAC) method, [11] and [5], *massless* marker particles are used to distinguish the phases. Thus, the marker particles are used solely to keep track of the phases and do not appear otherwise in the mathematical formulation of the problem. This is in contrast to the PIC method where the particles have mass assigned to them and are part of the formulation of the problem. This method also suffers from large memory requirements for book-keeping of the motion of a large number of particles.

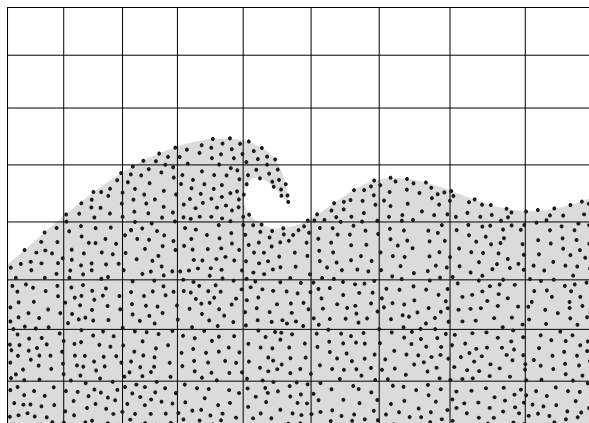


Figure 2.5: *MAC method.*

2.3.3 Volume of Fluid Method

In contrast to the PIC and MAC methods, the volume of fluid (VOF) method uses the volume fraction to mark the phases in the domain. Thus, it uses an Eulerian marking of the phases. Since the description of the phase-composition is associated with a fixed field instead of being attached to fluid elements, the method offers a simpler method of marking the phases. Additionally, since the method requires assigning only one variable to each cell in the mesh, it is also much less computationally expensive than MAC and PIC. But, with the

memory savings resulting from reducing the size of the data set tracking the phases comes also a loss in the information available. Most notably, when only the phase fraction of the phases is known in a cell containing part of the interface, there is indeterminacy regarding how the phases are arranged in the cell.

		0.16	0.46	0.19				
0.04	0.67	0.96	1	0.21	0.49	0.62	0.38	0.29
0.71	1	1	1	0.93	1	1	1	1
1	1	1	1	1	1	1	1	1
1	1	1	1	1	1	1	1	1
1	1	1	1	1	1	1	1	1

Figure 2.6: *VOF method.*

2.4 The VOF Method

The volume of fluid (VOF) method [12] is classified as an interface capturing method. The VOF method's most significant distinction from an earlier interface capturing method, the marker and cell (MAC) method [11], is that the former marks and follows the phases in an Eulerian manner while the latter relies on Lagrangian following of marker particles spread throughout one of the phases. Thus, the VOF method involves the solution of a single field equation for evolving the description of the location of the phases while the MAC method solves a large number of time-integration, kinematic equations for the marker particles. Of course, both methods also employ a common set of field equations as statements of conservation of mass and momentum.

Following the marking of the phases with the scalar volume fraction, the VOF method essentially treats the problem as that of the flow of a single fluid with variable properties. Thus, only a single pressure field, a single velocity field, etc. exist in the mathematical formulation of the problem in the VOF method.

The volume of fluid method uses the volume fraction of one of the fluids, in the case of a two-phase flow, to mark the phases. We define the scalar field of marker \mathbf{m} so that at time t_0 , $\mathbf{m} = 1$ at any *point* occupied by water and $\mathbf{m} = 0$ at any *point* occupied by air. The volume fraction of water, α , in a control volume V can then be defined as:

$$\alpha \equiv \frac{\int_V \mathbf{m} dV}{\int_V dV} \quad (2.1)$$

The point value of α can be seen to be equal to \mathbf{m} . However, the above definition will be useful later on in the report for control volumes of finite size.

2.4.1 Field Equations Governing The Flow

As explained earlier, the VOF method uses a single set of equations for describing the dynamics of the flow in the entire domain. Depending on which fluid occupies a point at any time during the solution, the appropriate fluid properties are substituted in the aforementioned equations. Neglecting the effect of surface tension in the problem at hand, the flow is governed by four statements of conservation of physical quantities. One equation describing conservation of mass and three equations describing conservation of momentum.

The conservation of mass is formulated by the continuity equation:

$$\frac{\partial \rho}{\partial t} + \nabla \cdot \rho \mathbf{U} = 0 \quad (2.2)$$

where \mathbf{U} is the velocity field and ρ is the density of the fluid. It should be noted that when this equation is written for a finite volume, the density will be non-constant even if each separate phase is incompressible. This is due to the fact that the phase constitution in a finite volume can change.

For the differential equations formulating Newton's second law, both phases are assumed to be Newtonian.

$$\rho \frac{\partial \mathbf{U}}{\partial t} + \rho \mathbf{U} \cdot \nabla \mathbf{U} = \nabla \cdot \sigma + \rho \mathbf{f} \quad (2.3)$$

where σ is the stress tensor and \mathbf{f} is the vector of the body force per unit mass, i.e. gravity.

By accounting for the phase discontinuity via variable properties, the VOF method introduces additional equations, in this case one, for keeping track of the advection of fluid properties within the Eulerian velocity field. In the current problem, this is done by introducing an equation describing the advection of the volume fraction of water α .

$$\frac{\partial \alpha}{\partial t} + \mathbf{U} \cdot \nabla \alpha = 0 \quad (2.4)$$

This equation is the mathematical formulation of the fact that the two phases are immiscible, and thus remain separate as the flow proceeds. It is thus a kinematic relation.

3 Numerical Model

The field equations governing the flow have no analytical solution except for a few very simple cases. Thus, numerical solutions are the method of choice for solving these equations. In order to attempt a numerical solution, the equations governing the flow need to be reformulated into algebraic equations that can be solved iteratively. The present chapter will introduce the reformulated form of the governing equations, suitable for numerical solutions.

3.1 Introduction

The local, instantaneous description of the dynamics of a flow field as depicted in a set of differential equations can actually be seen as the result of taking the limit of integral equations prescribed over a control volume as the size of that control volume approaches zero. This way of thinking about the equations of fluid flow seems all the more natural if one remembers that the conservation laws embodied in these equations are statements about observations made at *finite* length and time scales; i.e. conservation of mass, momentum and energy. In the most common current approach to the numerical solution of the equations of fluid flow, the *finite volume method*, the conservation equations are reformulated for control volumes of finite size. The problem domain is divided into a collection of small, non-overlapping control volumes and the unknown fields are assumed to have a simple analytical form in each such finite volume. An algebraic formulation of the problem is arrived at when the integrated statements of the conservation laws for all the finite volumes are patched together, with a finite number of unknown representative values to be calculated by minimizing a *residual*.

3.2 Integral Equations of Conservation

As already mentioned, the classical conservation laws governing the flow of fluids are statements about observations that have been seen to hold invariably. In an Eulerian framework, if \mathcal{V} is a control volume of finite size, a general statement of a conservation law for a scalar ϕ can be written as [25]

$$\frac{\partial}{\partial t} \int_{\mathcal{V}} \rho \phi \, d\mathcal{V} + \int_{\Omega} \rho \mathbf{U} \cdot \phi \hat{\mathbf{n}} \, dS = \int_{\Omega} \nabla \Gamma \phi \cdot \hat{\mathbf{n}} \, dS + \int_{\mathcal{V}} S_{\phi} \, d\mathcal{V} \quad (3.1)$$

where the left hand side is simply the substantial derivative of ϕ , Γ is the diffusion coefficient for property ϕ , Ω is the bounding surface of \mathcal{V} , and S_{ϕ} represents any source/sink of ϕ . Substituting 1 for ϕ in eq 3.1 results in the continuity equation. Substituting u , v and w would result in the three components of the momentum conservation equation. And finally, substituting α for ϕ yields the kinematic equation for the volume fraction.

To arrive at an algebraic formulation of eq 3.1, each field appearing inside an integral is assumed to have a certain closed, analytical form. Subsequently, the volume and surface integrals can be calculated. Eq 3.1 also involves a time derivative. To change this time derivative term to an algebraic form, the entire equation is time-integrated as in eq 3.2

$$\int \left(\frac{\partial}{\partial t} \int_{\mathcal{V}} \rho \phi \, d\mathcal{V} \right) dt + \int \left(\frac{\partial}{\partial t} \int_{\Omega} \rho \mathbf{U} \cdot \phi \hat{\mathbf{n}} \, dS \right) dt = \int \left(\frac{\partial}{\partial t} \int_{\Omega} \nabla \Gamma \phi \cdot \hat{\mathbf{n}} \, dS \right) dt + \int \left(\int_{\mathcal{V}} S_{\phi} \, d\mathcal{V} \right) dt \quad (3.2)$$

3.3 Discretization of The Geometry

The first step in a numerical solution using the finite volume method is the discretization of the problem domain. The domain is divided into a large number of non-overlapping control volumes over which the conservation equations are integrated. In this project, a variety of software packages were used for the creation of the mesh. The CAD model for the vehicle was worked on in a commercial software called ANSA. The cleaned CAD model was then fed into an open source meshing application, *snappyHexMesh*, which is part of the *OpenFOAM* software package. The resulting mesh contained about 32 million cells.

3.4 Discretization Schemes

As already mentioned, simple, closed-form algebraic formulae are assumed for the different fields in the finite volume method. With this approximation, the integrations in the general, integrated conservation equation, eq 3.2 can be carried out. The assumed behaviour of each term in the conservation equations is arguably the most crucial factor in the success or failure of a numerical solution using the finite volume technique. In the current project, the discretization schemes and other solver settings were changed as the solution advanced.

The solver was initially set up with first-order upwind scheme for the advection terms in the momentum and volume fraction equations. The temporal terms were discretized with the implicit, first-order scheme. These choices were made to ensure a robust solution in the initial stage where the rate of change in the solution was expected to be the greatest. As the solution proceeded, the time-step of the solver was increased in stages to reduce the execution time. The under-relaxation coefficients were also gradually increased. Once the solution approached a quasi-steady state, the spatial discretization scheme for the momentum equation was changed to bounded central differencing to improve the accuracy. The spatial discretization scheme for the volume fraction equation was also changed, to a compressive scheme to suppress diffusion of the large gradient close to the interface and confine the free surface to fewer cells. The SIMPLE algorithm was used for pressure-velocity coupling.

3.5 Boundary Conditions

No-slip boundary conditions were chosen for the body of the car and the ground. The top boundary was given a symmetry boundary condition, assuming that the boundary would be far enough for the streamlines to have become parallel to the x axis. The side walls of the domain were also given symmetry boundary conditions. In this case, the rationale was that this would approximate the behavior of the walls of the wading channel at the test site at Hällered by inhibiting normal velocity. This also meant that the effect of the boundary layer on the global flow was neglected as it was assumed to be negligible.

At the inlet to the domain, Dirichlet boundary conditions were set for the volume fraction equation to set the depth of water. The pressure was set to correspond to hydrostatic pressure. Dirichlet boundary conditions for the volume fraction and hydrostatic pressure specification were also used for the outlet. The velocity was also specified at the inlet. It should be mentioned that the results in the next chapter are from a case where this velocity was set to $2m/s$. Figure 3.1 shows a schematic of the numerical domain with the portion of the inlet for water highlighted.

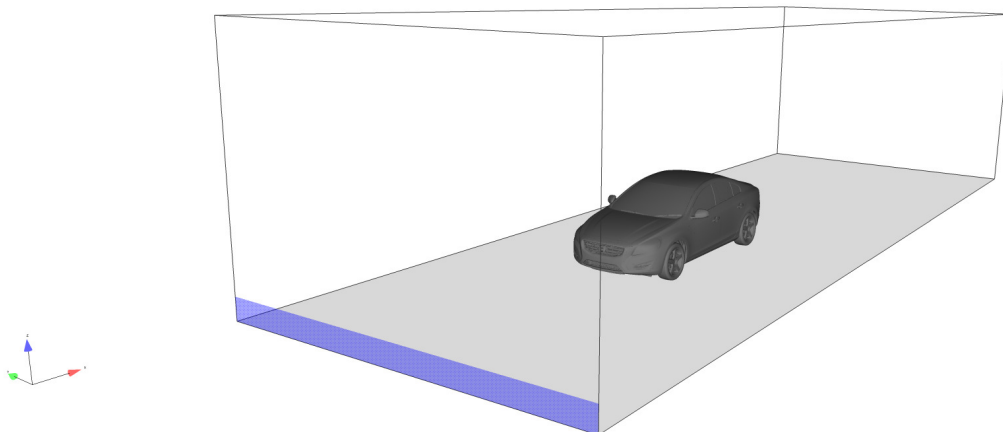


Figure 3.1: *Numerical domain.*

4 Results

4.1 Temporal Progression of the Solution

During the current project, different solver set-ups were tried to reach a robust method. Comparison of the resulting solutions revealed that the solution time interval in which the numerical solution moves from the initialized fields to the quasi-steady state is where the contrast between the different settings is the greatest, to the extent that the transient responses show quite distinct behaviors. Additionally, replication of the initial conditions between the numerical problem and the tests could not be achieved without introducing too many additional complications. For example, recreation of the entry of the vehicle into the wading channel would have required use of a dynamic mesh, which was not acceptable. This meant that no reliable testing data was available against which the numerical results could be compared. As a result, the solver settings during the transient phase of the numerical solution were decided on mainly to minimize the solution time without risking robustness. The rest of this chapter is solely concerned with the quasi-steady solution.

4.2 Quasi-steady Solution

As explained in Chapter 2, the VOF method treats a two-phase flow as the flow of a single fluid with varying properties. Accordingly, figure 4.1 shows the velocity field at the mid-plane of the channel. As can be seen, large gradients exist at the location of the change in properties. As expected, the low-density portion of the fluid accelerates while passing over the car and separates to form a low-velocity wake behind the car. However, this project is more concerned about the flow of the high-density portion of the fluid. From figure 4.1, it can be seen that there is a build up of water in front the vehicle, followed by acceleration to a higher velocity stream of lower depth.



Figure 4.1: *Contour of velocity magnitude at the mid-plane.*

The high-density portion of the fluid, representing water, can be isolated by only visualizing the $\alpha > 0.5$ portion of the domain. This has been done in 4.2. This figure also shows the reduction in water depth in the downstream direction. Because of the great difference in the magnitudes of most fields and properties between the high-density and the low-density portion of the fluid, in the rest of this chapter only the high-density phase will be visualized to improve clarity and readability.

Figure 4.3 shows the height contour of the free surface of water. It can be seen in this figure that there are surface waves upstream of the vehicle, which is expected since the flow is sub-critical. Also notable in the figure is the increasing angle of the contour lines with respect to the cross-channel direction. This indicates decreasing ratio between the velocity of surface waves and the mean flow which is accelerating. The figure also shows that there is a transition back to a higher depth downstream of the car.

To better examine the changes in the water depth, figure 4.4 shows a plot of the average depth of water at cross sections of the flow along the channel. The average depth was calculated by dividing the surface area of

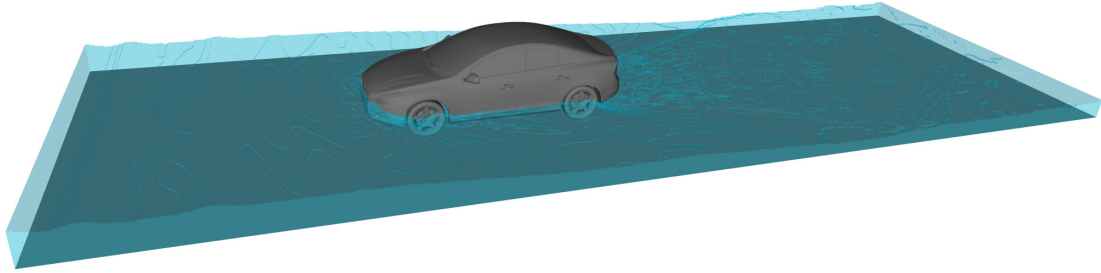


Figure 4.2: *High-density portion of the fluid isolated.*

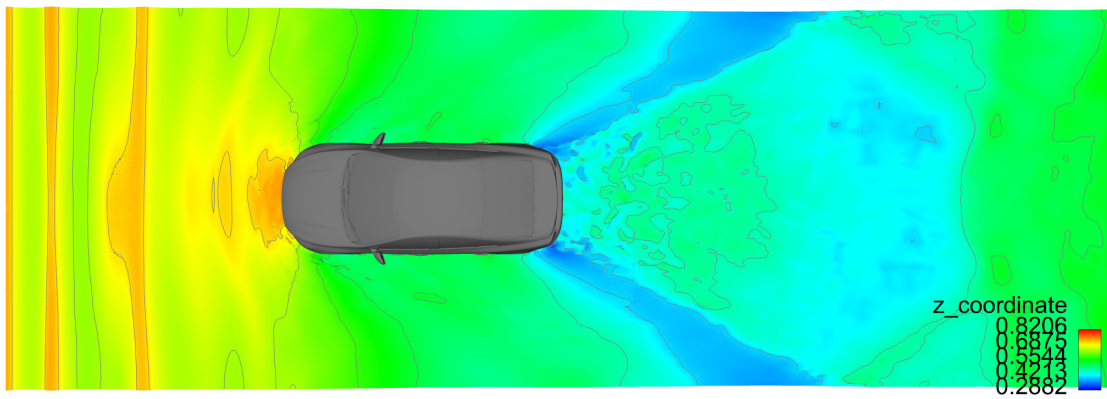


Figure 4.3: *Height contour of the free surface of water.*

the cross section by the constant channel width. The plot clearly shows the drop in depth as the water passes the car and the eventual depth recovery downstream of the car.

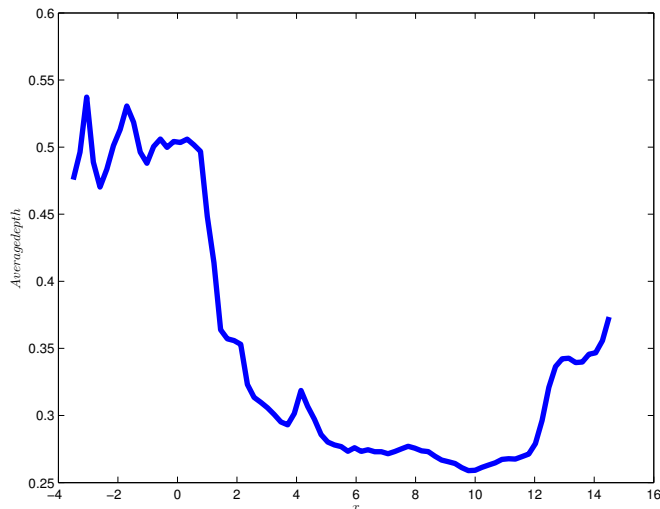
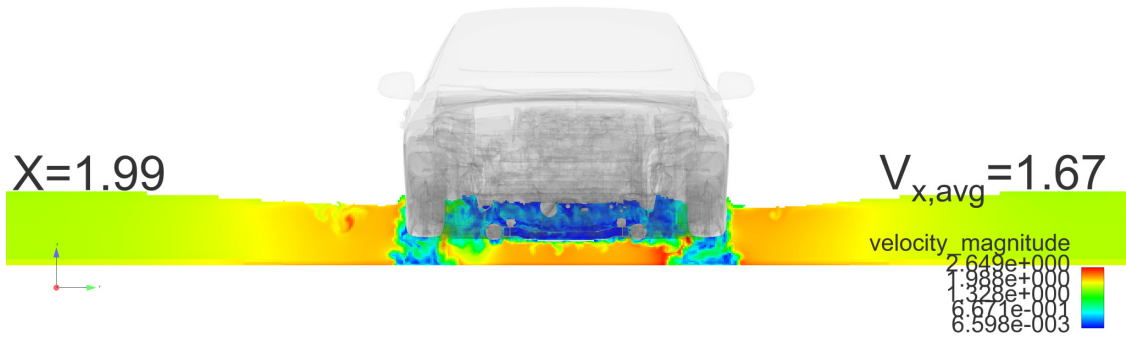


Figure 4.4: *Variation of average depth along the channel.*

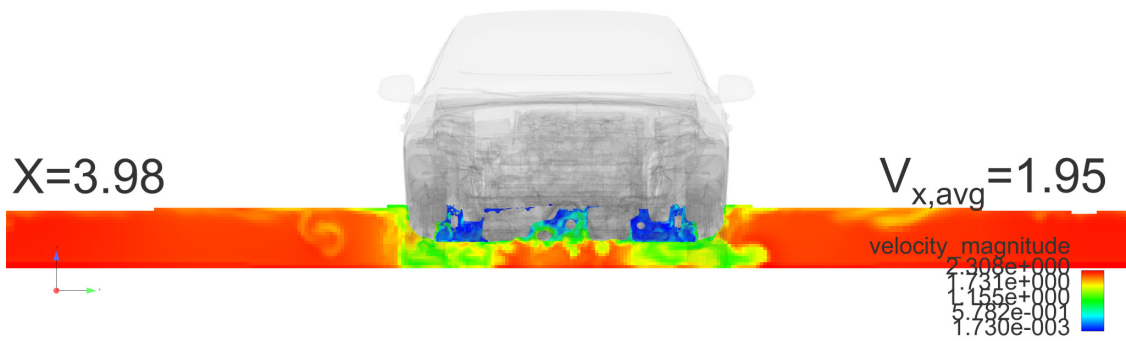
Figure 4.5a to 4.5f show contour plots of velocity magnitude at different cross section along the channel. The first notable feature of these figures is the manner in which the two streams of water, one passing under the car and one passing on the sides, merge downstream of the car. The higher-velocity stream from the sides penetrates the low-velocity flow from under the car, pushing the low velocity fluid upwards. This results in a low-velocity layer of fluid sitting on top of the mean flow further downstream and can be seen clearly in 4.6.

Figure 4.6 shows contours of the cross-channel velocity component at three locations along the channel. This figure further confirms the earlier observation about the behavior of the flow downstream of the car. It can be seen that following the increase in available flow area after the car, the two high-velocity streams from the sides rush towards the center and, as a result, displace the low-velocity water of the center stream to a layer on top. That the mixing of the two streams should happen in this particular manner can be attributed to the fact that the two streams on the sides have a greater depth and thus a higher pressure at the bottom of the channel; hence the direction of the cross-channel flow.

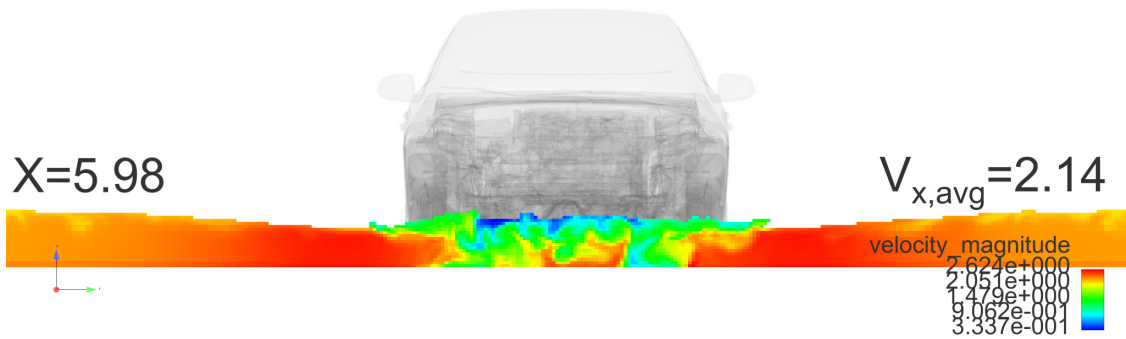
Figure 4.7 shows the velocity magnitude contour at the free surface of water. Together with figure 4.6, this figure also demonstrates the existence of a layer of low-velocity fluid on the surface of water downstream of the car. As can be seen, there is a sudden change in velocity magnitude at the surface, although no such change occurs in the mean velocity at the same location.



(a) $x = 2m$

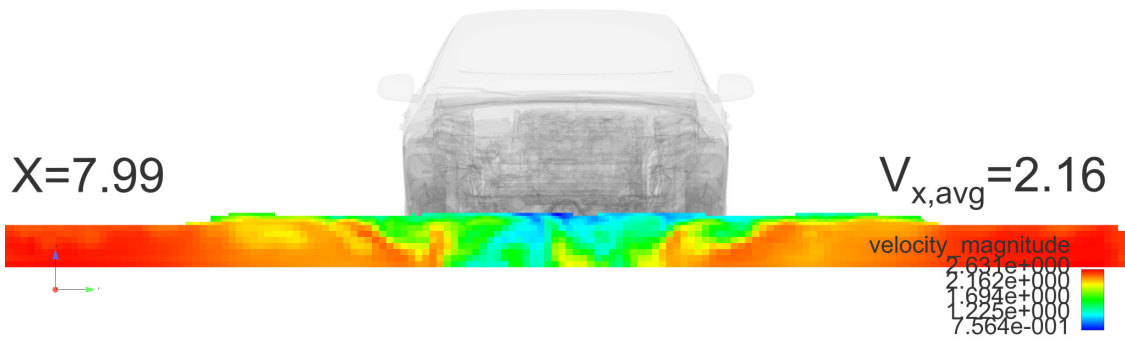


(b) $x = 4m$

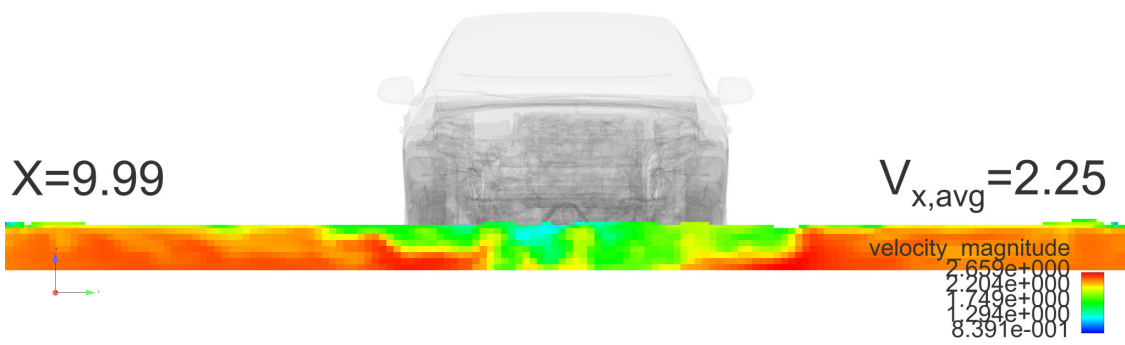


(c) $x = 6m$

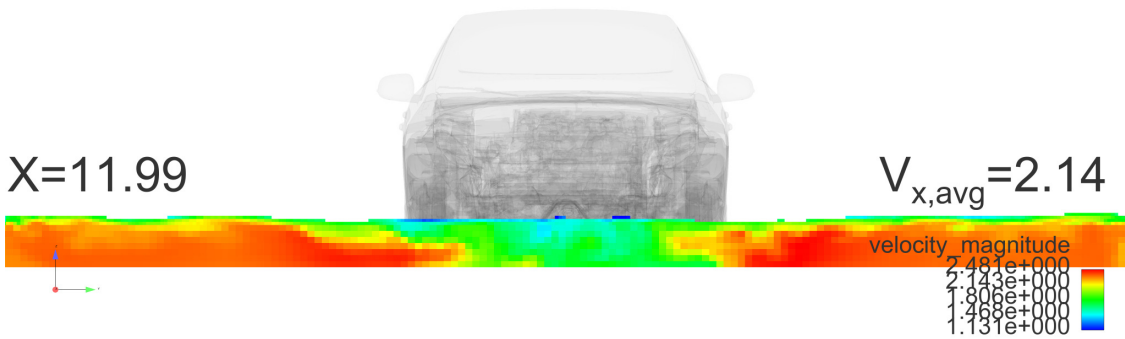
Figure 4.5: Velocity magnitude contours at various cross sections.(continued)



(d) $x = 8m$

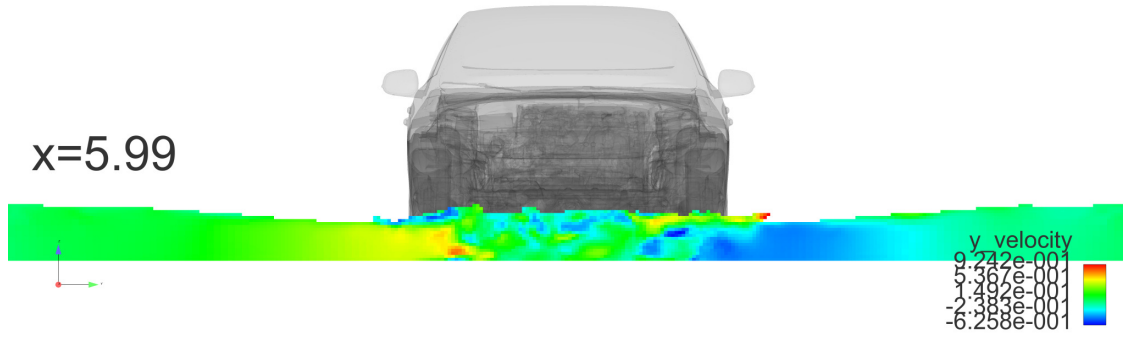


(e) $x = 10m$

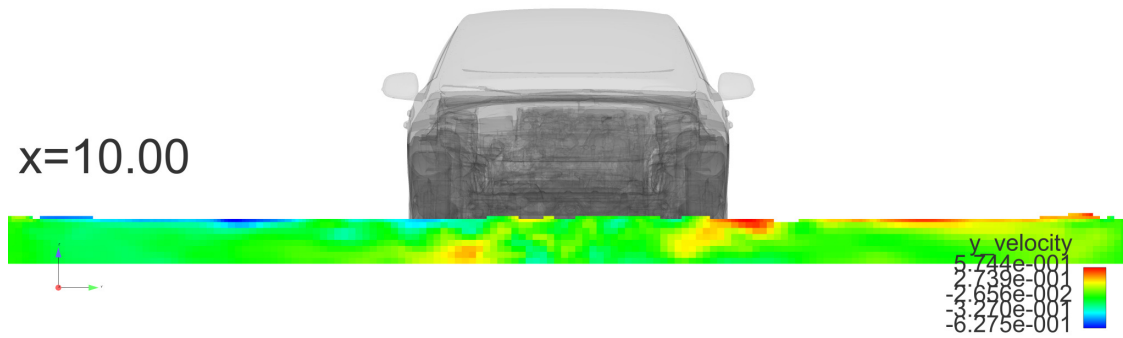


(f) $x = 12m$

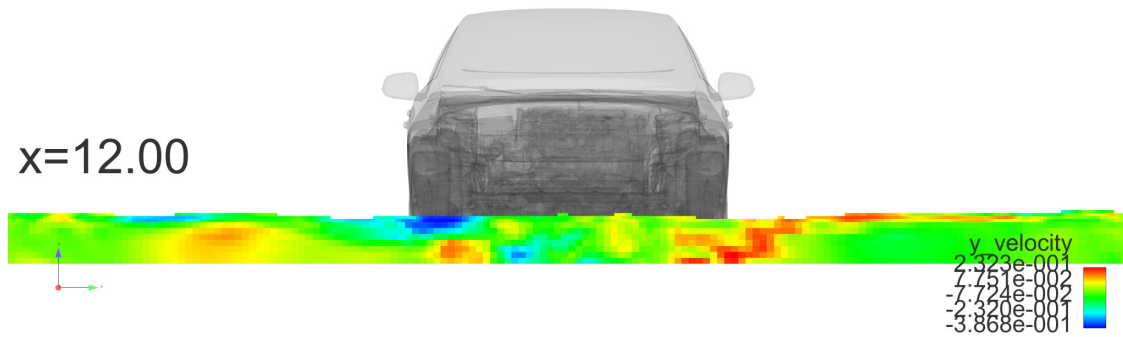
Figure 4.5: Velocity magnitude contours at various cross sections.



(a) $x = 6m$



(b) $x = 10m$



(c) $x = 12m$

Figure 4.6: *Contours of cross-channel velocity at various cross sections.*

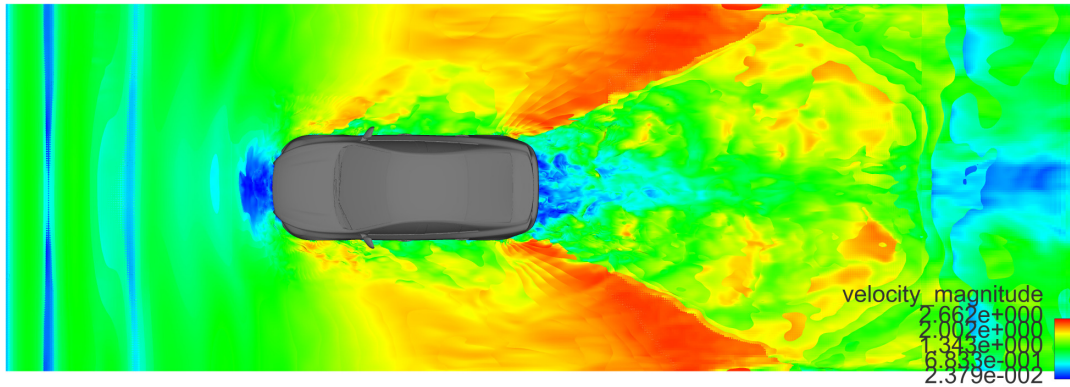


Figure 4.7: *Velocity magnitude contour at the free surface.*

4.3 Forces

One of the most valuable variables obtainable from the computational solution of wading is the net force exerted on the car. Because of the large density of water, the forces exerted on the car are significant and thus should be examined carefully. For example, since the vertical force exerted on the car reduces its effective weight, a wave hitting the car on the side could potentially wash it downstream. The same large vertical force exerted on the car also makes efficient and accurate calculation of forces a very hard task. Because of the large vertical forces acting on the car, there is a significant change in the state of the suspension system. This rising of the body of the car due to the force of water means that there is a change in the topology of the problem. However, because of the complexity of the geometry, dynamic implementation of this change of topology in the problem formulation is not feasible.

In this project, a simplified method was chosen to take the change of topology into account. It was assumed that the most dominant forces in the rearrangement of the suspension system are the buoyancy force trying to raise the car and the force from the springs acting against such a height raise. The springs were assumed to have a linear behavior and a simple mass-spring model with only one degree of freedom was chosen to represent the problem. The simplified model is depicted in figure 4.8.

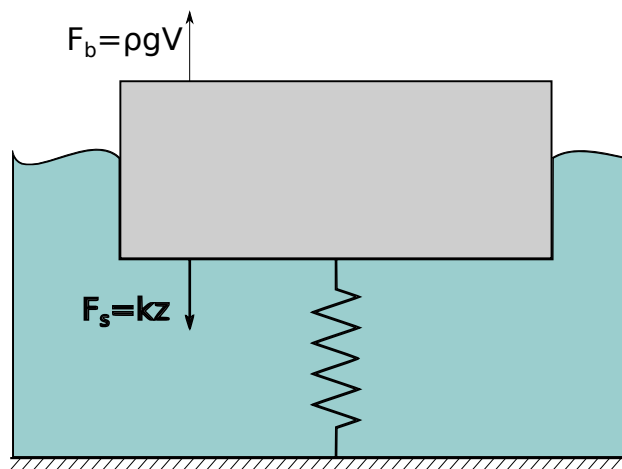


Figure 4.8: *Schematic of the simplified model for estimation of the height rise.*

The balance point for this simple system is where the height raise z satisfies the relation:

$$\rho g V(z) = k z \quad (4.1)$$

where z is the height raise measured from the normal balance point of the suspension system, ρ is the density of water, $V(z)$ is the volume of water displaced by the vehicle and k is the spring stiffness.

The buoyancy force was estimated by calculating the volume enclosed by the same CAD model used for the CFD simulation as a function of height. The CAD model was cut by a z -normal plane, as illustrated in figure 4.9 and the enclosed volume was calculated as a function of the z coordinate of the plane. A plot of the calculated volume against the z coordinate of the plane is shown in figure 4.10. The z coordinate of the plane in figure 4.10 should be taken to represent the depth of the water that the vehicle is wading through. It should be mentioned that the volume of the wheels and many drive-line components that are connected to the lower end of the suspension system was excluded from the calculations as they do not contribute to the buoyancy force acting to raise the car. Next, a simple algorithm was implemented to find the balance point between the buoyancy force and the spring force iteratively. Finally, the change in height of the car was accounted for in the CFD solution by reducing the *effective* depth of water in the CFD method by an amount equal to the height raise. In this way, the change in the state of the suspension system was roughly taken into account in the CFD solution.

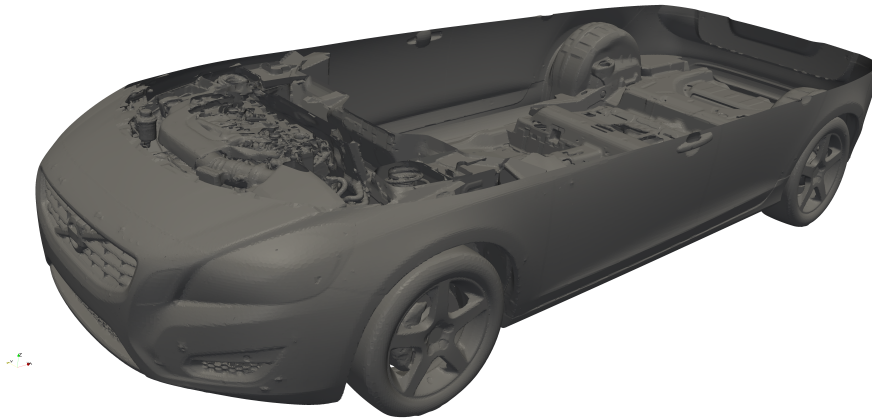


Figure 4.9: *Cut view of the car geometry.*

Figure 4.11 shows a comparison between the height raise calculated with the simplified method and measurements taken at the test facility at Hällered. The measured values are averaged values measured at the front and back wheels. The figure suggests that the simplified model overestimates height rise since the estimate is higher than the measured value at the lower speed. This can be attributed to the fact that the water depth, as the results from the previous section show, drops along the length of the car. Another point from the figure is the significant difference between measurements at different speeds. This suggests that the dynamic effects are not entirely negligible and that, naturally, they become more important with increasing speeds. The fact that dynamic forces are not completely negligible was not unexpected, however since the suggested method offers a very easy method of estimating the height raise a compromise was made. With accumulated measurement data, an additional empirical term can be added to the model to account for the dynamic effects.

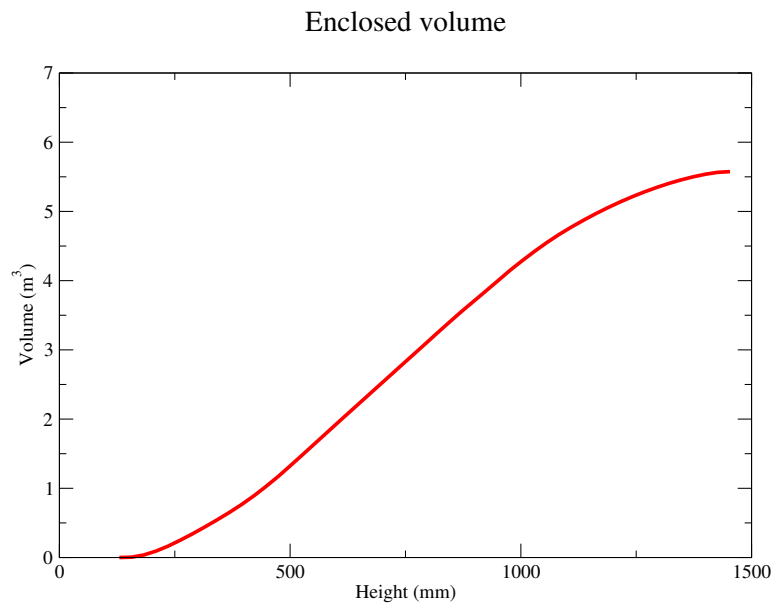


Figure 4.10: *Volume enclosed by the car.*

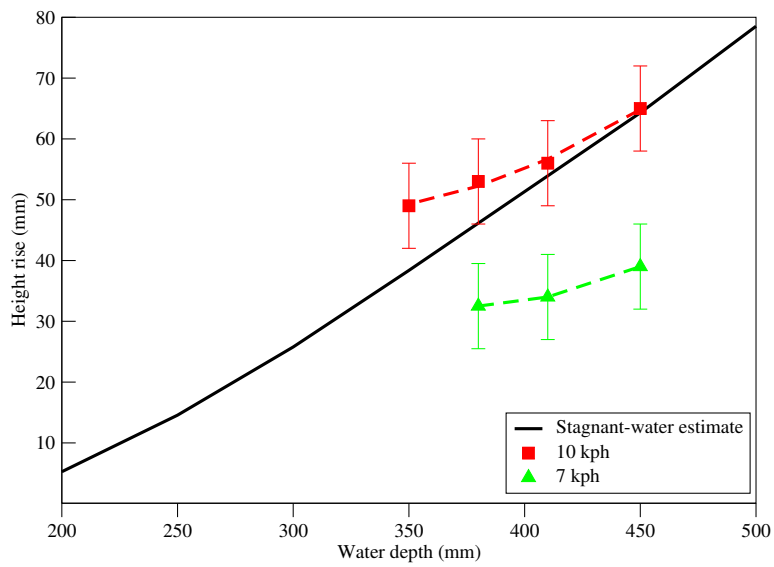


Figure 4.11: *Comparison of the estimated height raise with measurements.*

5 Conclusion

This chapter summarizes the project and provides suggestions for further work on the subject.

5.1 CFD Method

A method for carrying out numerical calculation of car wading was developed. The primary focus during the project was on the height of the wading line along the car as it determines whether or not water reaches sensitive sections such as the engine air inlet. The CFD method developed during the project is already in use at the time of this writing. Because of the complex nature of the flow, it is still required that both physical testing and numerical simulations are used to ensure satisfactory performance of a design. However, with a working method available, both physical testing procedures and the numerical method itself can be improved in a reciprocal manner if results from both are analyzed collectively. A list of possible ways for improving the computational method are presented:

- The log files created during the numerical solution can be analyzed and improvements can be made to reduce the execution time of the method. The calculations currently take tens of hours, depending on vehicle speed, water depth and other factors. As more data becomes available with the continued use of the method, improvements in execution time should be possible.
- The testing during the current project was carried out simultaneously with the calculations. With the subsequent analysis of the results, significant features were observed in the numerical solution that had not been sought after during the tests. These features should be examined during future tests as a means of qualitative verification of the numerical solution.

5.2 Forces

A simple method was suggested for estimation of the vertical force acting on the car and the subsequent rise in height. The method only considers the hydrostatic pressure force acting on the car and the spring force resisting changes in height. As the force exerted on the car has a complex dependence on the configuration of the flow and since the effective depth of water changes by the action of the water force on the car body, inclusion of such estimates in the CFD method itself were considered currently infeasible. The suggested method is particularly appealing as the same CAD model prepared for the CFD calculations can be used to estimate the buoyancy force. However, it was found that the simplified method overestimates the buoyancy force by an amount that can be attributed to the non-constant depth of water in the real flow, and other dynamic features of the flow not included in the model.

This simple estimation method can be improved by the addition of an empirical term to account for the dynamic effects. In this regard, the CFD results can provide a virtual testing platform for arriving at the empirical term.

5.3 Testing

Wading tests at the Hällered test site had not involved collection of quantitative data before the current project. During the project, elementary measurements were taken to estimate the height raise of the car. Despite the considerable cost of testing full-scale cars, the tests cannot be entirely abandoned since they represent the ultimate assurance against unacceptable performance. With such considerations, it can be argued that more value should be extracted from the investment in tests. In this regard, the computational method can be used, for example, to decide what data should be measured using standard design of experiment techniques.

References

- [1] R. Aris. *Vectors, tensors, and the basic equations of fluid mechanics*. New York: Dover Publications, 1989.
- [2] J. Billingham and A. C. King. *Wave motion*. Vol. 24. Cambridge University Press, 2001.
- [3] C. T. Crowe. *Multiphase flow handbook*. CRC, 2005.
- [4] B. J. Daly. A technique for including surface tension effects in hydrodynamic calculations. *Journal of Computational Physics* **4.1** (1969), 97–117.
- [5] B. J. Daly. Numerical Study of Two Fluid Rayleigh-Taylor Instability. *Physics of Fluids* **10** (1967), 297.
- [6] D. A. Drew and S. L. Passman. *Theory of multicomponent fluids*. Vol. 135. Springer, 1999.
- [7] M. W. Evans, F. H. Harlow, and E. Bromberg. *The particle-in-cell method for hydrodynamic calculations*. Tech. rep. DTIC Document, 1957.
- [8] J. H. Ferziger and M. Perić. *Computational methods for fluid dynamics*. Vol. 2. Springer Berlin etc, 1999.
- [9] D. Givoli. Non-reflecting boundary conditions. *Journal of Computational Physics* **94.1** (1991), 1–29.
- [10] V. R. Gopala and B. G. van Wachem. Volume of fluid methods for immiscible-fluid and free-surface flows. *Chemical Engineering Journal* **141.1** (2008), 204–221.
- [11] F. H. Harlow and J. E. Welch. Numerical Calculation of Time-Dependent Viscous Incompressible Flow of Fluid with Free Surface. *Physics of fluids* **8** (1965), 2182.
- [12] C. W. Hirt and B. D. Nichols. Volume of fluid (VOF) method for the dynamics of free boundaries. *Journal of computational physics* **39.1** (1981), 201–225.
- [13] J. M. Hyman. Numerical methods for tracking interfaces. *Physica D: Nonlinear Phenomena* **12.1** (1984), 396–407.
- [14] M. Ishii. Thermo-fluid dynamic theory of two-phase flow. *NASA STI/Recon Technical Report A* **75** (1975), 29657.
- [15] M. Ishii and T. Hibiki. *Thermo-fluid dynamics of two-phase flow*. Springer Science+ Business Media, 2011.
- [16] H. Jasak and H. Weller. Interface tracking capabilities of the inter-gamma differencing scheme. *Unpublished, February* **42** (1995).
- [17] D. B. Kothe and W. J. Rider. *A comparison of interface tracking methods*. Tech. rep. Los Alamos National Lab., NM (United States), 1995.
- [18] D. B. Kothe and W. J. Rider. Comments on modeling interfacial flows with volume-of-fluid methods. *submitted for publication* (1995).
- [19] P. Kundu and I. Cohen. *Fluid Mechanics. 2004*. Elsevier Academic Press, 2008.
- [20] S. Ozen Unverdi and G. Tryggvason. Computations of multi-fluid flows. *Physica D: Nonlinear Phenomena* **60.1** (1992), 70–83.
- [21] J. N. Reddy. *An introduction to continuum mechanics*. Cambridge University Press, 2007.
- [22] J. Romate. Absorbing boundary conditions for free surface waves. *Journal of computational Physics* **99.1** (1992), 135–145.
- [23] O. Ubbink and R. Issa. A method for capturing sharp fluid interfaces on arbitrary meshes. *Journal of Computational Physics* **153.1** (1999), 26–50.
- [24] O. Ubbink. “Numerical prediction of two fluid systems with sharp interfaces.” PhD thesis. Imperial College London (University of London), 1997.
- [25] H. K. Versteeg and W. Malalasekera. *An introduction to computational fluid dynamics: the finite volume method*. Prentice Hall, 2007.
- [26] G. H. Yeoh and J. Tu. *Computational techniques for multiphase flows*. Butterworth-Heinemann, 2009.